Inorganic Chemistry

Article

pubs.acs.org/IC

# Tetrathiafulvalene-Triazine-Dipyridylamines as Multifunctional Ligands for Electroactive Complexes: Synthesis, Structures, and Theoretical Study

Diana G. Branzea, Arnaud Fihey, Thomas Cauchy, Abdelkrim El-Ghayoury,* and Narcis Avarvari*

LUNAM Université, Université d'Angers, CNRS UMR 6200, Laboratoire MOLTECH-Anjou, 2 bd Lavoisier, 49045 Angers Cedex, France

Supporting Information

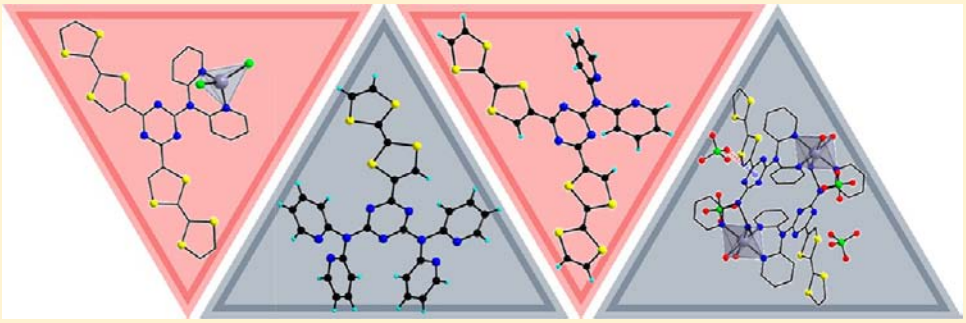

**ABSTRACT:** The electroactive ligands (2,4-bis-tetrathiafulvalene[6-(dipyridin-2′-ylamino)]-1,3,5-triazine) $TTF_2$-tz-dpa (**1**) and (2-tetrathiafulvalene[4,6-bis-(dipyridin-2′-ylamino)]-1,3,5-triazine) TTF-tz-$dpa_2$ (**2**) have been synthesized by palladium cross-coupling catalysis, and the single crystal X-ray structure for **1** was determined. In the solid state the TTF and triazine units are practically coplanar and short intermolecular S···S contacts are established. Two neutral and one tetracationic Zn(II) complexes, formulated as ($TTF_2$-tz-dpa)$ZnCl_2$ (**3**), [$ZnCl_2$(TTF-tz-$dpa_2$)Zn($H_2O$)$Cl_2$] (**4**), and {[($H_2O$)$_2$Zn(TTF-tz-$dpa_2$)]($ClO_4$)$_2$}$_2$ (**5**) have been crystallized and analyzed by single crystal X-ray analysis. A peculiar feature is the evidence for anion-$\pi$ interactions, as shown by the short Cl···triazine and O(perchlorate)···triazine distances of 3.52 and 3.00 Å, respectively. A complex set of intermolecular $\pi$···$\pi$, S···S, and hydrogen bonding interactions sustain the supramolecular organizations of the complexes in the solid state. Electronic absorption spectra provide evidence for the intramolecular charge transfer from TTF to triazine, also supported by time-dependent density functional theory (TD DFT) calculations.

## INTRODUCTION

1,3,5-Triazine derivatives have been known for a long period of time in organic chemistry. They have found widespread applications as 2,4,6-mono, di- or trisubstituted, symmetrical and non symmetrical compounds bearing different substituents.[1] The preparation of these compounds relies on the differential reactivity of trichlorotriazine (cyanuric chloride) in successive nucleophilic substitution steps.[2] Some of the prepared derivatives have been utilized as biologically active compounds.[1a,3] In the past recent years, triazine based compounds have been used as active materials for electroluminescence devices,[4] donor−acceptor redox-active materials,[5] nonlinear optics,[6] cooperative two-photon absorption materials,[7] and as ferromagnetic coupling unit.[8]

In addition, the 1,3,5-triazine (tz) ring has been extensively utilized in coordination chemistry as a building block for symmetrical and non symmetrical multicoordination sites ligands. Hence, the large majority of the coordinating units attached to the 2,4,6 positions of the 1,3,5-triazine are N-donor sites, while the triazine nitrogen atoms are involved in only few cases in the coordination of metallic centers. Accordingly, $C_3$ symmetrical tritopical ligands such as 2,4,6-tris(4-pyridyl)-1,3,5-triazine (tpt),[9] 2,4,6-tris(di-2-pyridylamino)-1,3,5-triazine (dipyatriz),[10] or 2,4,6-tris(di-2-pycolylamino)-1,3,5-triazine[11] have been extensively utilized in diverse metallic complexes with various architectures and properties, while among other related less employed, since they are subjected to hydrolysis with some metal halides, one can find 2,4,6-tris(2-pyridyl)-1,3,5-triazine,[8a,12] 2,4,6-tris(2-pyrimidyl)-1,3,5-triazine,[12a,13] or 2,4,6-tris-(4-((pyridine-4-ylthio)methyl)-phenyl)-1,3,5-triazine.[14] Moreover, the triazine moiety as evidenced by its relatively accessible one-electron reduction potential,[15] possesses electron-acceptor properties, which can be tuned by the different substituents.[16] Such a $\pi$-electron-poor character makes it a suitable candidate for relatively rare and nevertheless very interesting $\pi$-anion supramolecular interaction.[11a,17] It has also been utilized in the construction of donor−acceptor systems where the donor is a tetrathiafulvalene (TTF) moiety.[16c,18] It is also well established that TTF and its derivatives have attracted much interest

**Received:** May 27, 2012
**Published:** July 16, 2012

   dx.doi.org/10.1021/ic301117h | *Inorg. Chem.* 2012, 51, 8545−8556

because of their electron-donating ability and redox properties, making them valuable precursors for a whole range of applications.[19] They have been widely used, for example, as donor components in the preparation of molecular conductors and superconductors.[20] One of the ongoing challenges in this field concerns the preparation of multifunctional materials which can exhibit synergy or coexistence between two or more properties, such as conductivity and magnetism, luminescence, chirality, spin-crossover, and so forth.[21] To address this challenge, considerable efforts have been devoted in associating TTF moieties, via spacers or bonds, with metal containing fragments, exerting both a structural and a functional role. Accordingly, various organic mono- or polydentate ligands, and their corresponding electroactive metal complexes have therefore been reported.[22] For example, metal complexes of TTF-phosphines,[23] -oxazolines,[24] -dithiolates,[25] -acetylacetonates,[26] -pyridines,[27] -bipyridines,[28] and, more recently, -Schiff bases[29] have been synthesized.

As mentioned above, the $C_3$ symmetric ligand dipyatriz, containing the triazine ring as backbone and three di-2-pyridylamine (dpa) chelating units, has been used in a whole series of metal complexes.[10] To obtain functional complexes that combine intriguing structures, from a crystal engineering point of view,[30] and interesting properties, we decided to covalently associate triazine-dpa fragments with TTF units, to take advantage of their individual features, within multifunctional precursors. We report herein the synthesis and characterization of two unprecedented $(dpa)_n$-triazine-$(TTF)_m$ ($n = 1$, $m = 2$ or $n = 2$, $m = 1$) chelating ligands, together with neutral and cationic Zn(II) complexes.

## RESULTS AND DISCUSSIONS

**Synthesis of the ligands and complexes.** The protocol followed for the synthesis of the new ligands $TTF_2$-tz-dpa **1** and TTF-tz-$dpa_2$ **2** is summarized in Scheme 1. The selective

**Scheme 1. Synthesis of the Ligands 1 and 2**

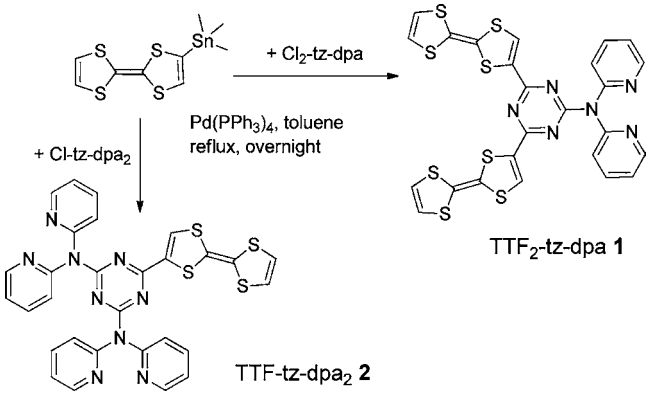


reactivity found with 2,4,6-trichloro-1,3,5-triazine (cyanuric chloride) and dipyridylamine allowed us the preparation of the dichlorinated $Cl_2$-tz-dpa and the monochlorinated Cl-tz-$dpa_2$ precursors, which were then reacted with 1 or 2 equiv of TTF-$SnMe_3$ under the Stille coupling conditions, using $Pd(PPh_3)_4$ as catalyst in toluene, to afford **1** and **2** in good yields (73% and 81%, respectively), after chromatographic workup.

Single crystals of both ligands **1** and **2** were obtained by slow evaporation of solvents from a mixture of dichloromethane and hexane. However, only the crystals of **1** were of suitable quality for a single crystal X-ray analysis (vide infra).

The propensity of dpa type ligands to form complexes with the Zn(II) ion has been proven.[31] Therefore, as a first coordination chemistry study with the new electroactive ligands, the affinity of **1** and **2** toward Zn(II) has been investigated. Accordingly, the ligand **1** was reacted with 1 equiv of zinc chloride ($ZnCl_2$) in a dicloromethane/acetonitrile mixture to afford the complex **3** formulated as ($TTF_2$-tz-dpa)$ZnCl_2$. By a similar procedure, the ligand **2** was reacted with 2 equiv of $ZnCl_2$ to form the dinuclear complex **4** $[ZnCl_2(TTF\text{-tz-}dpa_2)Zn(H_2O)Cl_2]$, while by reaction with 1 equiv of zinc perchlorate $Zn(ClO_4)_2$, a discrete dimeric structure formulated as $\{[(H_2O)_2Zn(TTF\text{-tz-}dpa_2)](ClO_4)_2\}_2$ (**5**) was formed.

**Description of the Crystal Structures.** The ligand **1** crystallizes in the monoclinic space group $P2_1/a$, with one independent molecule in the unit cell. The fragment formed by the two TTF units and the triazine ring is almost planar, the dihedral angles between least-squares planes of the triazine and the adjacent dithiole rings amounting to 2.38° (S1S2) and 4.37° (S5S6), respectively (Figure 1).

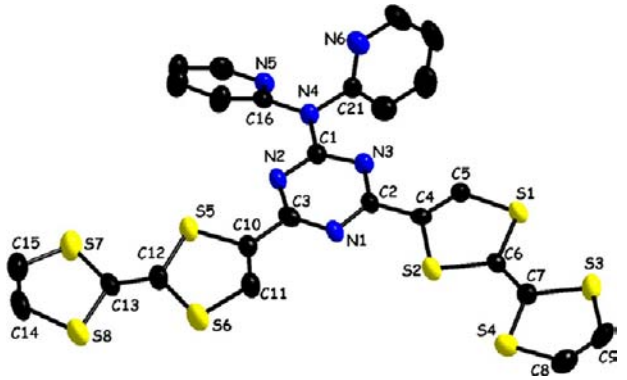


**Figure 1.** Molecular structure of **1** in the solid state. Ellipsoids have been drawn at 50% probability. Hydrogen atoms have been omitted.

C=C and C−S distances are typical for neutral TTFs (Table 1). Worth noting is the N4−C1 distance of 1.376(5) Å, much

**Table 1. Selected Bond Lengths (Å) in 1**

| 1 | | | |
|---|---|---|---|
| N4−C1 | 1.376(5) | C4−C5 | 1.328(6) |
| N4−C16 | 1.432(5) | C4−C2 | 1.468(6) |
| N4−C21 | 1.445(5) | C3−C10 | 1.468(6) |
| N1−C2 | 1.338(5) | C10−C11 | 1.323(6) |
| N1−C3 | 1.346(5) | C6−C7 | 1.344(6) |
| N3−C2 | 1.328(5) | C13−C12 | 1.337(6) |
| N3−C1 | 1.339(5) | | |

shorter than the N4−$C_{py}$ distances (1.432(5) Å for N4−C16 and 1.445(5) Å for N4−C21), indicating a stronger $\pi$ donation from the amine to the triazine ring than toward the two pyridine rings. In the crystal the packing is mainly governed by sulfur−sulfur interactions, one molecule being involved in short S···S contacts[22−28] with other six of its neighbors generating two-dimensional (2D) layers (Figure 2). The solid state architecture is also reinforced by the presence of intra-


dx.doi.org/10.1021/ic301117h | Inorg. Chem. 2012, 51, 8545−8556

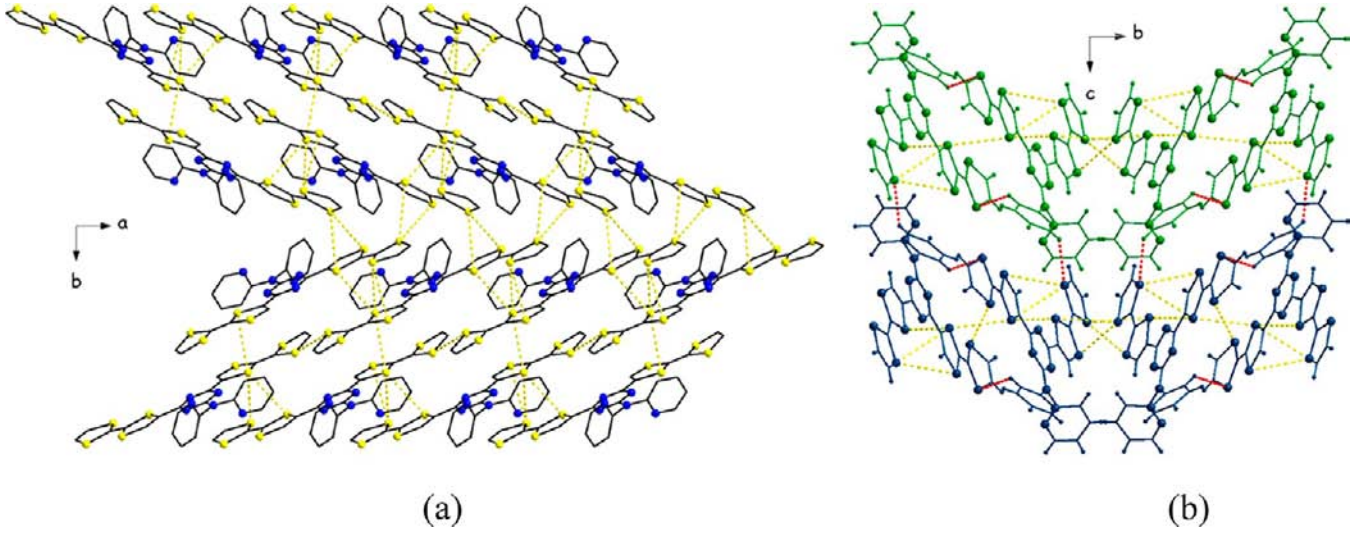


**Figure 2.** Crystal packing in the structure of **1**: layer generated by short S···S contacts (yellow dashed lines) in the *ab* plane (a); side view (*bc* plane) of two layers represented in different colors connected by short C−H···S contacts (red dashed lines) (b). Distances (Å): S1···S3(0.5+*x*, 0.5−*y*, *z*) 3.56; S2···S3(0.5+*x*, 0.5−*y*, *z*) 3.73; S2···S5(−1+*x*, *y*, *z*) 3.60; S4···S5(−1+*x*, *y*, *z*) 3.77; S4···S6(−1+*x*, *y*, *z*) 3.80; S5···S5(1−*x*, −*y*,2−*z*) 3.77; S7···S7(2−*x*, −*y*,2−*z*) 3.64.

(H17···S8 2.96 Å) and interlayer short C−H···S contacts (H17···S8 2.84 Å).[32]

The complex **3** crystallizes in the triclinic system, space group $P\bar{1}$, with one independent molecule in the unit cell. As in the free ligand, the two TTF units and the 1,3,5-triazine ring are almost planar (Figure 3), with dihedral angles dithiole-triazine

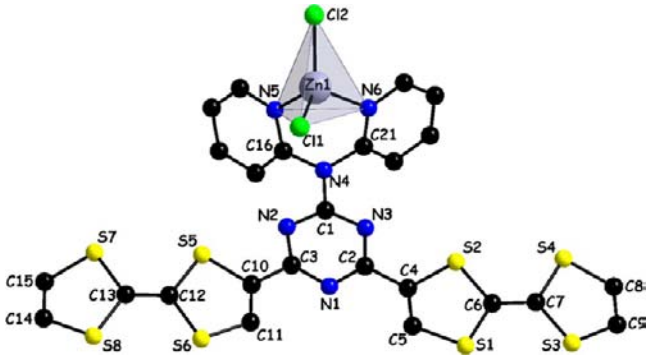


**Figure 3.** Molecular structure of **3** in the solid state, with an emphasis on the zinc coordination sphere. Hydrogen atoms have been omitted.

of 1.97° (S1S2) and 4.55° (S5S6), thus suggesting a certain conjugation between them. The zinc ion is tetracoordinated, its distorted tetrahedral coordination sphere being formed by two pyridine nitrogen atoms provided by the dpa unit and two chlorine atoms. Bond lengths within the TTF and triazine units do not differ substantially with respect to those in the free ligand (Table 2). Once again, the values for C=C and C−S bonds are typical for neutral TTFs, while the distance N4−C1 (1.383(4) Å) is much shorter than N4−C21 (1.438(4) Å) and N4−C16 (1.434(5) Å), thus suggesting an electron density transfer from the amine toward the triazine cycle.

The two TTF units of the molecule stack in an offset manner giving rise to molecular columns running along the *a* axis (Figure 4). The columns are interconnected by short S···S contacts (S3···S8 3.47 Å) into supramolecular layers.

Furthermore, the pyridine rings N5 belonging to neighboring sheets are involved in offset $\pi-\pi$ stacking[33] (centroid···centroid 3.80 Å) to achieve a three-dimensional (3D) architecture (Figure 5). The 3D supramolecular network is also reinforced by unconventional hydrogen bonding established by the two chlorine atoms and the $H_{TTF}$.[34] These contacts have values in the 2.73−2.87 Å range (Table 3).

The complex **4** crystallizes in the triclinic system, space group $P\bar{1}$, with one independent molecule in the unit cell, and its single-crystal X-ray analysis reveals that it is a dinuclear Zn(II) complex formulated as $[ZnCl_2(TTF\text{-}tz\text{-}dpa_2)Zn(H_2O)Cl_2]$, where the ligand **2** acts as bridge with its two coordinating dipyridine-amine moieties (Figure 6).

Once again, the TTF-triazine fragment is basically planar, with a dihedral angle of 12.47° between the two units. A peculiar feature of the complex **4** is represented by the presence of the zinc ions in two different stereochemistries. Indeed, the Zn1 center is tetracoordinated within a distorted tetrahedral environment, while Zn2 is pentacoordinated, its coordination sphere comprising, apart from the two pyridine nitrogen atoms and the two chlorine atoms as in the case of Zn1, also an oxygen atom from a coordinating water molecule. The calculated value of the $\tau$ parameter ($\tau = [(\alpha - \alpha')/60]$, where $\alpha$ and $\alpha'$ are the *transoid* angles formed by the metal ion and the donor atoms within the basal plane), a parameter generally used to assess the distortion between the square pyramidal and trigonal bipyramidal stereochemistries,[35] is 0.957, suggesting a slight distortion from the trigonal bipyramidal geometry. Furthermore, we can assume that the geometry around Zn2 is affected by the presence of an intramolecular $\pi$-anion interaction between the chlorine atom Cl3 coordinated to zinc and the electron-deficient triazine ring, as suggested by the Cl3···triazine centroid distance of 3.52 Å.[10c] Moreover, the Zn2−Cl3 distance (2.249(1) Å) is significantly longer than Zn2−Cl4 (2.219(1) Å), as a consequence of this interaction. The latter compare with the Zn1−Cl bond lengths values of the second coordinative unit (Table 2). Evidences for such interactions are rather scarce compared to $\pi$-cation interactions, although they are of great importance in the field of supramolecular chemistry and molecular recognition.[36] Note that C=C and C−S bond lengths are in the typical range for


dx.doi.org/10.1021/ic301117h | *Inorg. Chem.* 2012, 51, 8545−8556

**Table 2. Selected Bond Lengths (Å) and Angles (deg) in 3–5**

| 3 | | 4 | | 5 | |
|---|---|---|---|---|---|
| | | Bond Length (Å) | | | |
| C1–N3 | 1.336(4) | C4–C3 | 1.343(6) | C3–C4 | 1.325(8) |
| C1–N2 | 1.335(4) | N2–C8 | 1.322(6) | C5–C6 | 1.342(8) |
| C1–N4 | 1.383(4) | N2–C9 | 1.331(5) | C6–C7 | 1.454(7) |
| C2–N1 | 1.327(5) | N3–C9 | 1.338(5) | C7–N1 | 1.331(6) |
| C2–N3 | 1.340(5) | N3–C7 | 1.339(6) | C7–N3 | 1.341(7) |
| C2–C4 | 1.472(5) | N1–C8 | 1.336(5) | C8–N2 | 1.333(6) |
| C3–N1 | 1.331(5) | N1–C7 | 1.340(5) | C8–N1 | 1.335(6) |
| C3–N2 | 1.348(4) | N4–C8 | 1.390(5) | C9–N2 | 1.329(6) |
| C3–C10 | 1.458(5) | N7–C9 | 1.376(6) | C9–N3 | 1.342(6) |
| C4–C5 | 1.340(5) | N7–C25 | 1.427(6) | C9–N7 | 1.391(6) |
| C6–C7 | 1.331(6) | N7–C20 | 1.446(6) | C10–N4 | 1.438(6) |
| C11–C10 | 1.347(5) | C6–C5 | 1.331(6) | C15–N4 | 1.441(6) |
| C12–C13 | 1.319(6) | C6–C7 | 1.459(6) | C20–N7 | 1.433(6) |
| C16–N4 | 1.434(5) | Zn1–N6 | 2.071(4) | C25–N7 | 1.443(6) |
| C21–N4 | 1.438(4) | Zn1–N5 | 2.076(4) | N5–Zn1 | 2.121(4) |
| N5–Zn1 | 2.085(3) | Zn1–Cl1 | 2.203(1) | N6–Zn1 | 2.145(4) |
| N6–Zn1 | 2.062(3) | Zn1–Cl2 | 2.208(1) | N8–Zn1$^a$ | 2.147(4) |
| Cl1–Zn1 | 2.212(1) | Zn2–N9 | 2.107(4) | N9–Zn1$^a$ | 2.114(4) |
| Cl2–Zn1 | 2.194(1) | Zn2–N8 | 2.173(4) | O9–Zn1 | 2.235(4) |
| | | Zn2–Cl4 | 2.219(1) | O10–Zn1 | 2.178(4) |
| | | Zn2–Cl3 | 2.249(1) | Zn1–N9$^a$ | 2.114(4) |
| | | Zn2–O1 | 2.421(5) | Zn1–N8$^a$ | 2.147(4) |
| | | Angles (deg) | | | |
| N6—Zn1—Cl2 | 112.54(10) | N6–Zn1–N5 | 88.66(15) | N9$^a$–Zn1–N5 | 175.84(16) |
| N5—Zn1—Cl2 | 114.23(9) | N6–Zn1–Cl1 | 112.43(11) | N9$^a$–Zn1–N6 | 95.33(16) |
| N6—Zn1—Cl1 | 116.92(10) | N5–Zn1–Cl1 | 108.95(11) | N5–Zn1–N6 | 88.82(16) |
| N5—Zn1—Cl1 | 107.56(9) | N6–Zn1–Cl2 | 115.96(11) | N9$^a$–Zn1–N8$^a$ | 87.26(16) |
| Cl2—Zn1—Cl1 | 115.18(5) | N5–Zn1–Cl2 | 107.95(11) | N5–Zn1–N8$^a$ | 92.00(16) |
| N6—Zn1—Cl2 | 112.54(10) | Cl1–Zn1–Cl2 | 118.41(7) | N6–Zn1–N8$^a$ | 99.31(16) |
| | | N9–Zn2–N8 | 85.67(16) | N9$^a$–Zn1–O10 | 90.76(15) |
| | | N9–Zn2–Cl4 | 115.30(12) | N5–Zn1–O10 | 89.41(15) |
| | | N8–Zn2–Cl4 | 97.60(11) | N6–Zn1–O10 | 88.62(15) |
| | | N9–Zn2–Cl3 | 116.73(12) | N8$^a$–Zn1–O10 | 171.98(16) |
| | | N8–Zn2–Cl3 | 98.80(12) | N9$^a$–Zn1–O9 | 86.97(16) |
| | | Cl4–Zn2–Cl3 | 126.24(7) | N5–Zn1–O9 | 88.90(15) |
| | | N9–Zn2–O1 | 87.05(18) | N6–Zn1–O9 | 173.95(16) |
| | | N8–Zn2–O1 | 172.72(17) | N8$^a$–Zn1–O9 | 86.38(16) |
| | | Cl4–Zn2–O1 | 85.69(13) | O10–Zn1–O9 | 85.75(16) |
| | | Cl3–Zn2–O1 | 84.32(14) | | |

$^a$1–$x$, 1–$y$, –$z$.

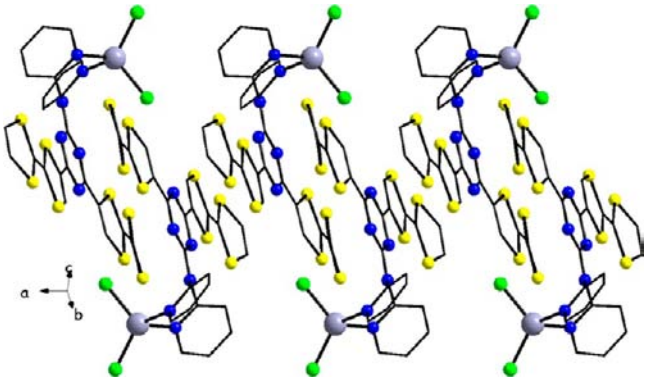

**Figure 4.** Crystal packing in **3**: perspective view of a supramolecular column generated by the stacking of the neighboring TTF units.

neutral TTFs. As in the case of the complex **3**, crystal packing reveals the presence of short S···S contacts (S2···S3 3.92 Å, S1···S4 3.86 Å) generated by the stack of two neighboring TTF units (centroid···centroid 3.86 Å). These supramolecular dimers are involved in offset $\pi$–$\pi$ stacking through the N6 pyridyl rings (centroid···centroid 3.45 Å) (Figure 7). The solid state architecture is also sustained/reinforced by the presence of unconventional C–H···Cl hydrogen bonds with distances varying in the range of 2.74–2.95 Å (Table 3).

Since the ligand **2** is ditopical, with two chelating units in *meta* position, its reaction with metal centers having at least four available coordination sites could, in principle, lead to the formation of either coordination polymers or discrete metallacycles. To evaluate this opportunity, but also the occurrence of intermolecular $\pi$-anion interactions, by the use of a noncoordinating anion, **2** was reacted with 1 equiv of $Zn(ClO_4)_2$. The resulting complex **5** crystallizes in the monoclinic space group $P2_1/n$ as discrete dimers, formulated as $\{[(H_2O)_2Zn(TTF\text{-}tz\text{-}dpa_2)](ClO_4)_2\}_2\cdot 4H_2O$, where the ligands bridge two zinc ions through two dipyridine-amine


dx.doi.org/10.1021/ic301117h | Inorg. Chem. 2012, 51, 8545–8556

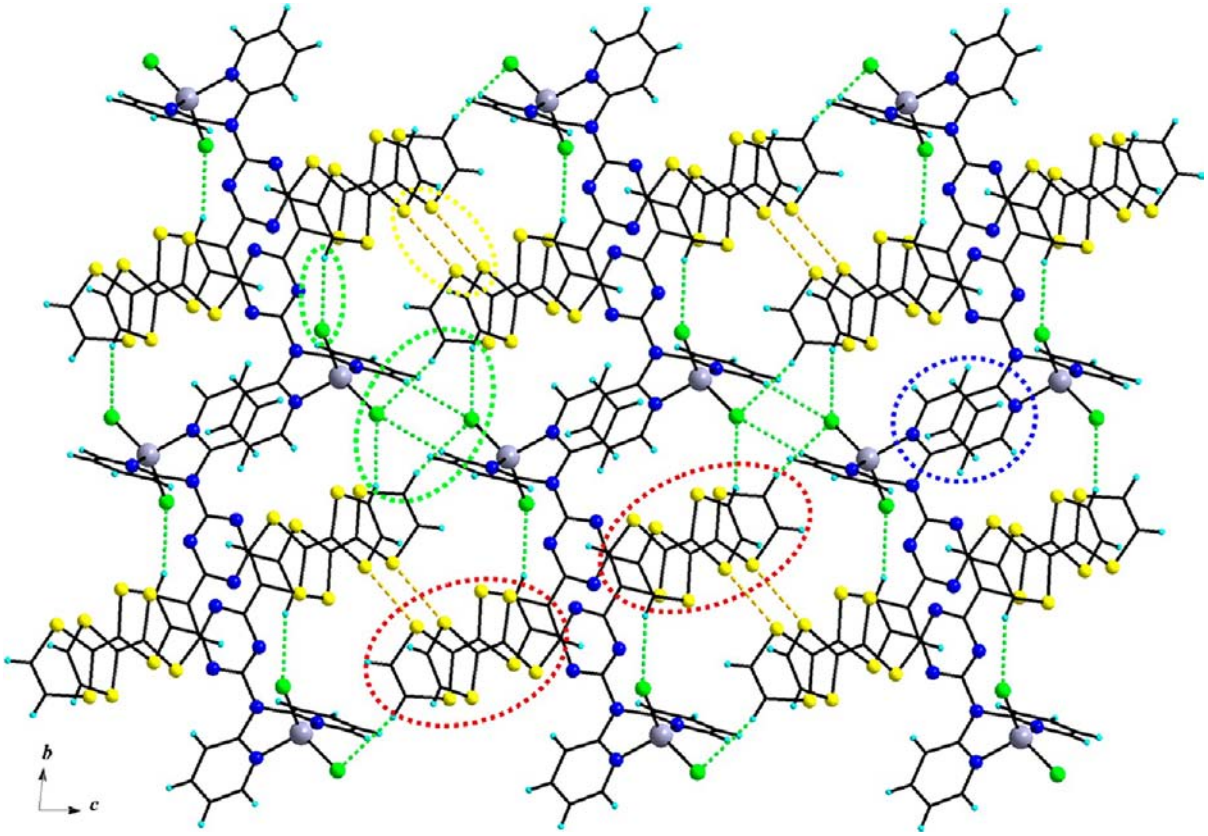


**Figure 5.** Crystal packing in **3** highlighting all the supramolecular interactions: the stacking between the TTF units (red), the S···S short contacts (yellow), the offset $\pi-\pi$ stacking between the pyridine rings (blue), and the unconventional C−H···Cl hydrogen bonds (green).

**Table 3. Intermolecular Hydrogen Bonds (Å) in 3−5**

| 3 | | 4 | | 5 | |
|---|---|---|---|---|---|
| H11···Cl1 | 2.73 | H28···Cl2 | 2.92 | O10···O2A | 2.74 |
| H9···Cl2 | 2.79 | H15···Cl2 | 2.74 | O10···O7 | 2.89 |
| H15···Cl2 | 2.87 | H29···Cl2 | 2.95 | O9···O1A | 2.66 |
| H25···Cl2 | 2.83 | H25···Cl3 | 2.86 | O6···O2A | 2.79 |
| | | | | O4···O2A | 2.93 |

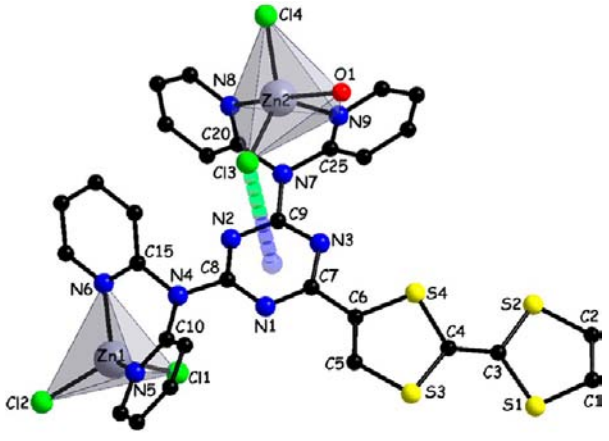


**Figure 6.** Molecular structure of **4** in the solid state, with an emphasis on the coordination spheres. The $\pi$-anion interaction is highlighted.

chelating moieties (Figure 8). Note that similar dimeric iron and cobalt metal complexes have been obtained with the precursor Cl-tz-dpa$_2$.[37] The asymmetric unit consists of half of the cationic complex, two perchlorate anions, and two crystallization water molecules.

The TTF···triazine dihedral angle (14.11°) is slightly larger than in the previous complex, but still the two moieties are practically coplanar. Apart from the four nitrogen atoms provided by two dipyridine-amine chelating units belonging to two different ligands, two oxygen atoms from water molecules coordinated in *cis* position complete the octahedral environment around the two zinc cations. The position occupied by the Cl1 perchlorate anions in the crystal structure is not random, but very likely the consequence of the $\pi$-anion supramolecular interaction that exists between the perchlorate anion Cl1 and the electron deficient triazine ring. This observation is supported by the short distance (3.00 Å) between the triazine centroid and the O1 atom of the Cl1 perchlorate ion,[10f] and also by the longer bond length Cl1−O1 (1.421(5) Å) than the other Cl−O distances. C═C and C−S bond lengths are in the usual range for neutral TTFs (Table 2). The coordinating water molecules together with the crystallized water molecules and the perchlorate anions are involved in a network of hydrogen bonds (Table 3) connecting the dimers in the *bc* crystallographic plane into a supramolecular layer (Figure 9).

The oxygen atoms of the different water molecules and perchlorate anions are involved in hydrogen bonds which define an infinite helical chain running along the *b* crystallographic axis (Figure 10). Within the crystal, there are both right-handed (*P* chirality) and left-handed (*M* chirality) of such hydrogen bonded helical chains disposed in an alternative manner (Figure 10).


dx.doi.org/10.1021/ic301117h | *Inorg. Chem.* 2012, 51, 8545−8556

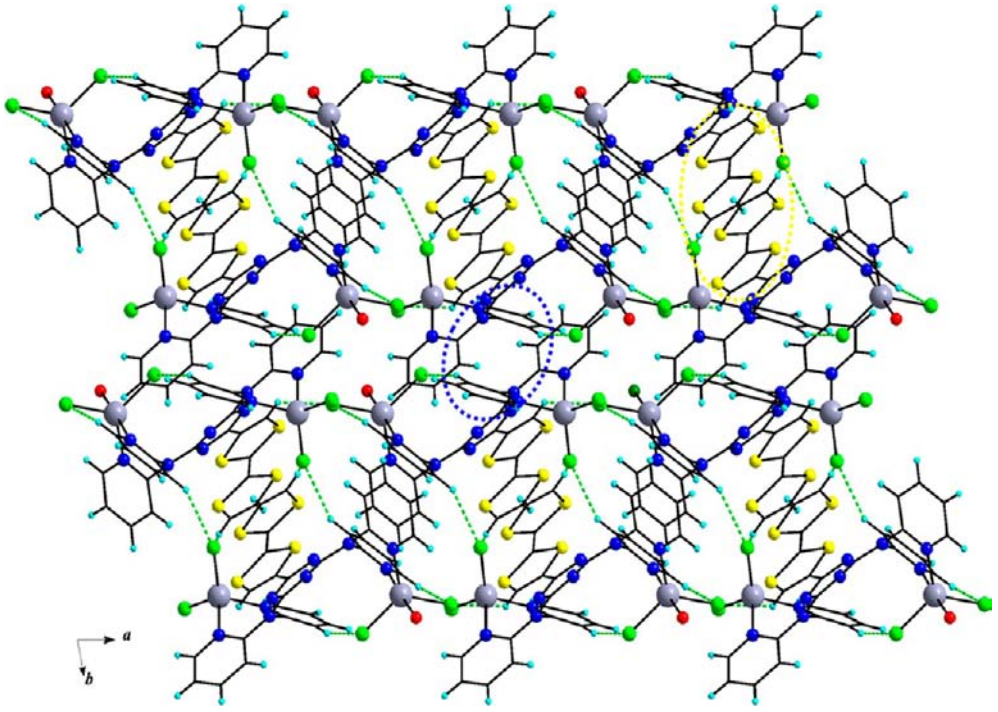

**Figure 7.** Crystal packing in **4**; the stacking between the TTF units (yellow) and the offset $\pi-\pi$ stacking between the pyridine rings (blue) are highlighted.

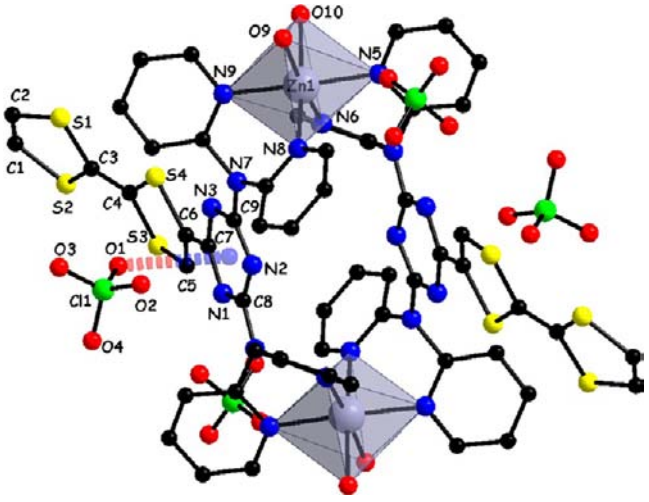


**Figure 8.** Molecular structure of **5** in the solid state, showing the $\pi$-anion interaction.

Other unconventional short contacts such as C−H···S (Supporting Information), linking the neighboring supramolecular layers, reinforce the solid state architecture. The dimeric nature of the complex is very likely preserved in solution, as demonstrated by electron spray mass spectrometry analysis, showing a peak resulting from the loss of the four coordinated water molecules (two for each Zn center) and one perchlorate anion.

**UV−visible Spectroscopy.** To study and to evidence the occurrence of donor-to-acceptor intramolecular charge transfer (ICT), UV−visible electronic absorption spectra for the ligands **1** and **2** were recorded in acetonitrile solution at room temperature (Figure 11), and were then compared with the theoretical spectra provided by time-dependent density functional theory (TD DFT) calculations on the optimized geometries (vide infra). The intense electronic absorption bands located at $\lambda$ = 299 and 286 nm, respectively, with shoulders at around 315−320 nm, contain typical $\pi\rightarrow\pi^*$ transitions of TTFs, besides triazine-dpa centered transitions.[38] The broad bands, especially for **1**, observed in the visible region at $\lambda_{max}$ = 504 nm for **1** and $\lambda_{max}$ = 473 nm for **2** are very likely characteristic of the intramolecular charge transfer (ICT) from the TTFs to the electron-accepting triazine units and are responsible for the dark red-violet color of these compounds. Similar ICT bands, also supported by TD DFT calculations, were previously described for TTF-triazine-methoxy derivatives.[16c] However, in the latter the equivalent ICT transitions were observed at $\lambda_{max}$ = 530 nm for $TTF_2$-tz-OMe and $\lambda_{max}$ = 492 nm for TTF-tz-$(OMe)_2$, that is, red-shifted by about 20−30 nm when compared to **1** and **2**, respectively. This feature is very likely related to a more important $\pi$ donation of the dpa group than the methoxy group toward the triazine ring, which promotes a stronger destabilization of the triazine based lowest unoccupied molecular orbital (LUMO), and thus larger gaps between the highest occupied molecular orbital (HOMO) and the LUMO in the dpa series described herein.

Upon complexation of **1** and **2** with $ZnCl_2$ the resulting electronic absorption spectra are similar to those of the free ligands (Supporting Information), showing a negligible effect of the coordinated metallic fragment on the ICT band. This feature is not surprising, since the pyridine rings of the dpa fragments, responsible for the coordination of the metallic fragments, are not involved in the composition of the HOMO and LUMO orbitals and do not directly interact with them. However, mass spectra of the complexes clearly indicate their stability in solution. On the contrary, the absorption spectrum of the dimeric tetracationic complex **5** is quite different from the one of the free ligand **2** and the neutral complex **4** (Supporting Information), since besides the intense band at $\lambda$ = 302 nm due to $\pi\rightarrow\pi^*$ transitions of TTFs, a new band,


dx.doi.org/10.1021/ic301117h | *Inorg. Chem.* 2012, 51, 8545−8556

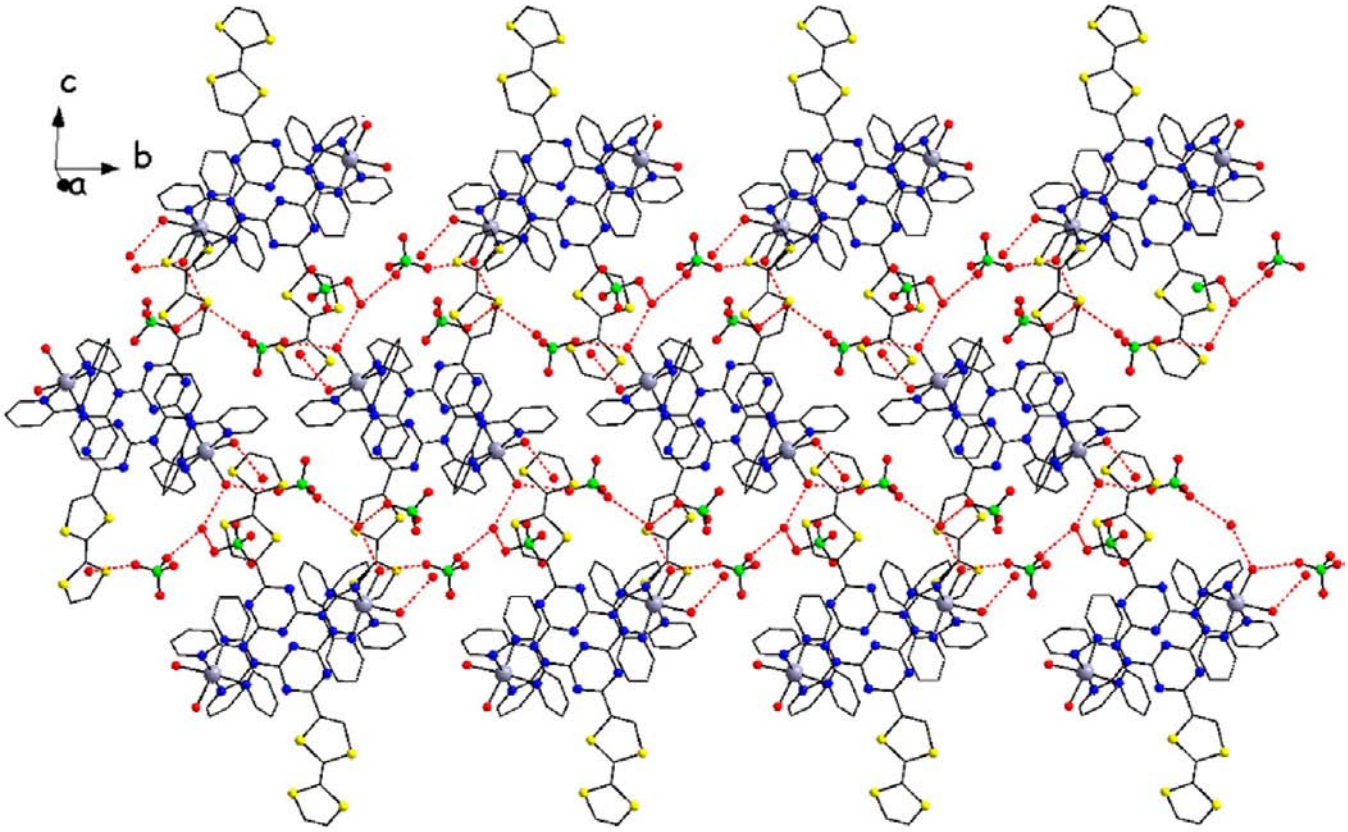


**Figure 9.** Perspective of the supramolecular layer generated by hydrogen bonding in **5**.

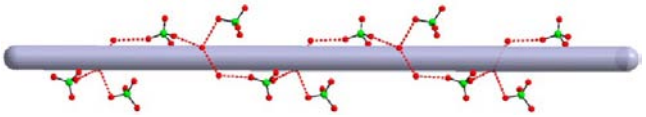

**Figure 10.** *P* helical chain formed by hydrogen bonds between the water molecules and perchlorate ions in **5**.

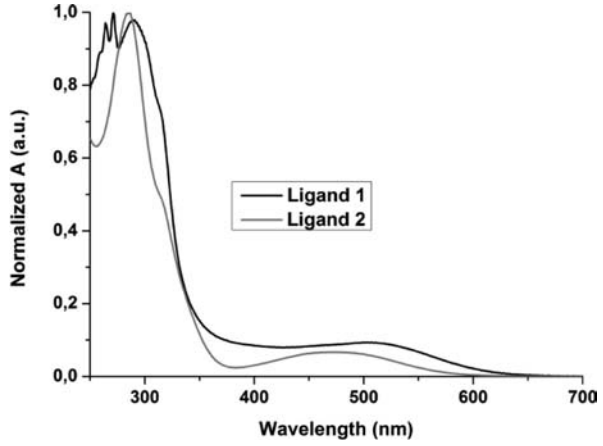


**Figure 11.** UV−vis spectra of $TTF_2$-tz-dpa (**1**) ($\lambda_{max}$ = 504 nm) and TTF-tz-$dpa_2$ (**2**) ($\lambda_{max}$ = 473 nm) (acetonitrile, $c = 5.10^{-5}$ M).

probably due to the triazine-dpa fragment and/or LMCT, appears now at $\lambda$ = 373 nm, while the ICT band centered at $\lambda$ = 500 nm is very large and less intense.

**Electrochemistry.** The electrochemical behavior of the ligands and of the complexes was investigated by cyclic voltammetry. The measurements in the case of the ligand **1** show two reversible oxidations at +0.45 V and +0.89 V (Table 4) that are anodically shifted when compared to the ones of the free TTF (0.37 and 0.67 V vs SCE)[19a] because of the presence of the electron deficient triazine ring. The signals are rather broad, possibly because of the two successive one-electron oxidation processes occurring at very close potentials. This behavior is similar to the one observed for the $TTF_2$-triazine-OMe donor.[16c] In the negative region, the irreversible reduction peak at around −1.43 V is attributed to the reduction of the triazine ring. The electrochemical behavior of the resulting Zn complex **3** is quite similar, thus suggesting a negligible influence of the metal coordination on the oxidation potential of the TTF units, a situation often encountered when the ligand and the TTF are well separated.[22a] The ligand **2** oxidizes at slightly higher potential (+0.50 V) when compared to **1** (+0.45 V). Moreover, the irreversible reduction of the triazine ring occurs at lower potential (−1.75 V) when compared to that of **1**, in agreement with the relative energy levels of the triazine based LUMO orbitals. Both zinc complexes **4** and **5** present reversible oxidations and irreversible

**Table 4. Oxidation Potentials of the Compounds 1−5 in V vs SCE**

| compound | $E_{1/2}^1$ | $E_{1/2}^2$ | $E_{red}$ |
|---|---|---|---|
| **1** | 0.45 | 0.89 | −1.43 |
| **2** | 0.50 | 0.95 | −1.75 |
| **3** | 0.42 | 0.88 | −1.47 |
| **4** | 0.47 | 0.92 | −1.75 |
| **5** | 0.48 | 0.86 | −1.84 |


dx.doi.org/10.1021/ic301117h | *Inorg. Chem.* 2012, 51, 8545−8556

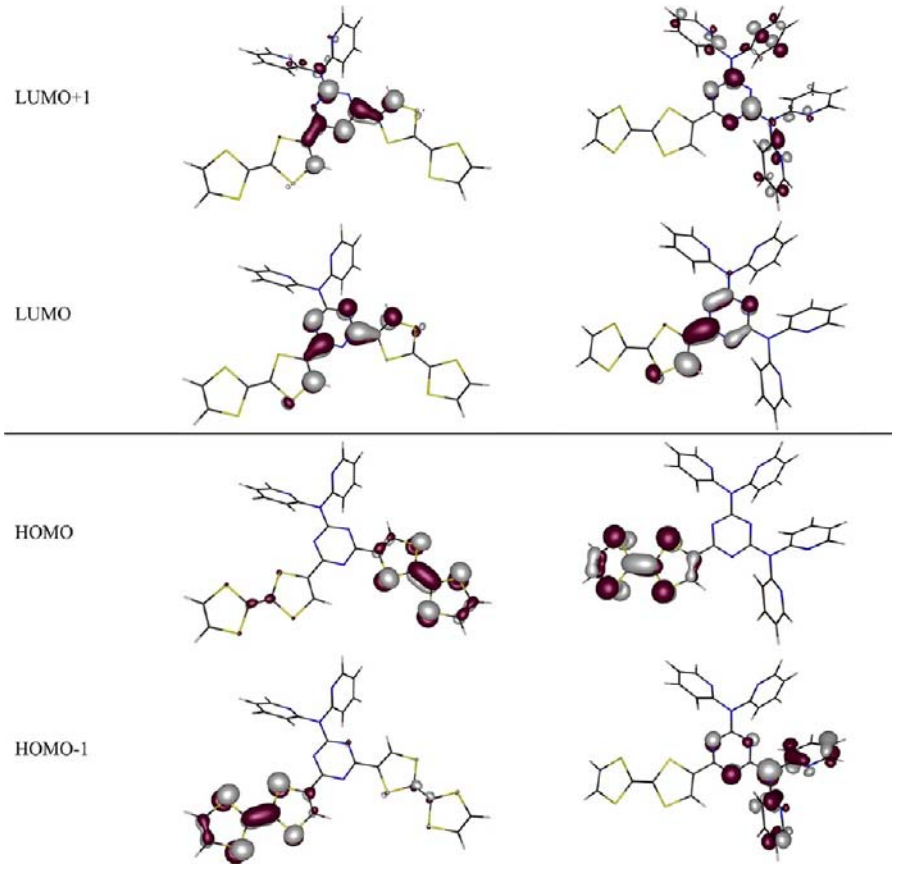


**Figure 12.** Frontier orbitals representation for **1** (left) and **2** (right) with an isovalue of 0.05.

reduction in the same potential range as the free ligand, very likely because of the large distance between the TTF and the coordinating units, as noticed also for the complex **3**.[22a]

**Theoretical Calculations.** Theoretical calculations at the density functional theory (DFT) level allowed first the optimization of the equilibrium gas phase geometries of **1** and **2**. Theoretical bond lengths and angles closely match the experimental X-ray values in the case of **1** (Supporting Information), showing for both **1** and **2** coplanar conformations between TTF and triazine units. As previously noticed in the case of $TTF_2$-tz-OMe donor,[16c] the highest occupied orbitals HOMO and HOMO-1 for **1** develop on each TTF unit, respectively, and are practically degenerate (Figure 12). The LUMO, rather low in energy (− 2.19 eV), is of $\pi$ type and has a pronounced triazine character, yet containing important contributions from the adjacent dithiole halves. The HOMO−LUMO gap amounts to 2.74 eV, superior to the one calculated in the case of $TTF_2$-tz-OMe (2.42 eV),[16c] and thus in agreement with the bathochromic shift of the ICT band in the latter when compared to **1**. Note also the LUMO+1, of $\pi$ type, developed essentially on the triazine ring and the adjacent dithiole halves. The molecular orbitals diagram for **2** shows, as expected, a TTF based HOMO, and a LUMO consisting in a combination of triazine and adjacent dithiole orbital fragments. The LUMO level is now higher in energy (− 1.81 eV), while the HOMO−LUMO gap increases to 3.06 eV, and thus the ICT band is expected to occur at higher energy for **2** than for **1**.

Moreover, vertical excitations energies were calculated by TD DFT on the optimized geometries of **1** and **2** to characterize the nature of the electronic transitions observed in the UV−vis spectra. In the case of **1** the low energy ICT band results from two energetically close HOMO−LUMO (594 nm) and HOMO-1−LUMO (570 nm) (Figure 13, Table 5) transitions,

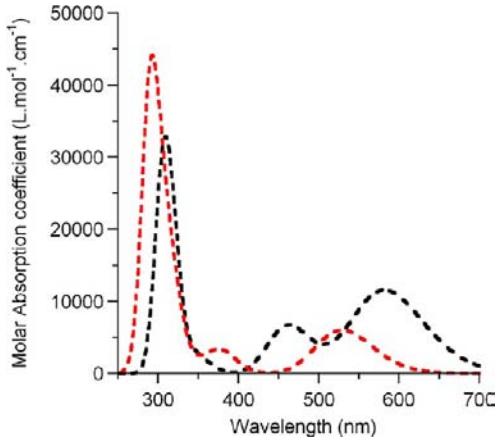


**Figure 13.** Theoretical absorption spectra of **1** (black dashed line) and **2** (red dashed line).

the calculated values being in agreement with the experimental one. Then, the next calculated band at 463 nm is due to a combined HOMO/HOMO-1−LUMO+1 transition and very likely contributes to the broadness and peculiar shape of the first experimental band observed in the UV−vis spectrum of **1** (see Figure 11).

The ICT band for **2** is calculated at 529 nm (Figure 13, Table 6), as HOMO−LUMO transition, with a relative weaker oscillation factor than the ICT in **1**, when compared to the


dx.doi.org/10.1021/ic301117h | Inorg. Chem. 2012, 51, 8545−8556

Table 5. TD-DFT Calculated Energies and Assignment of the Most Pertinent Low-Lying Electronic Singlet Excitations of 1

| wavenumber ($cm^{-1}$) | $\lambda$ (nm) | osc. | assignment | transition |
|---|---|---|---|---|
| 16830 | 594 | 0.09 | TTF→Tz/TTF | HOMO→LUMO (97%) |
| 17551 | 570 | 0.08 | TTF→Tz/TTF | HOMO-1→LUMO (95%) |
| 21575 | 463 | 0.07 | TTF→Tz/TTF | HOMO/-1→LUMO+1 (95%) |
| 31890 | 314 | 0.08 | TTF→TTF/Tz | HOMO→LUMO+14/+15/+11/+12/+13/+16 (55%) |
| 32093 | 312 | 0.09 | TTF→TTF/Tz | HOMO-1→LUMO+14/+10/+13 (45%) |
| 32556 | 307 | 0.29 | TTF→TTF/Tz | HOMO-3→LUMO (69%) |

Table 6. TD-DFT Calculated Energies and Assignment of the Most Pertinent Low-Lying Electronic Singlet Excitations of 2

| wavenumber ($cm^{-1}$) | $\lambda$ (nm) | osc. | assignment | transition |
|---|---|---|---|---|
| 18892 | 529 | 0.08 | TTF→Tz/TTF | HOMO→LUMO (99%) |
| 26462 | 378 | 0.04 | TTF→Tz/dpa | HOMO→LUMO+1 (95%) |
| 31324 | 319 | 0.08 | Tz/dpa→Tz | HOMO-1/-2→LUMO (95%) |
| 33039 | 303 | 0.07 | TTF→TTF/Tz | HOMO→LUMO+15/+10/+8/+11/13 (74%) |
| 34028 | 294 | 0.11 | TTF→TTF/Tz | HOMO→LUMO+11/+10/+14/+12 (82%) |
| 34468 | 290 | 0.39 | TTF→TTF/Tz | HOMO-3→LUMO (31%) |
| | | | | HOMO→LUMO+10/+11/+18 (27%) |

most intense transition, hence in agreement with the experimental spectra. The calculated red shift of the ICT in **2** with respect to that in **1** also parallels the experimental one.

## CONCLUSIONS

During this work we succeeded in the preparation of two multifunctional ligands based on TTF as electron donating unit, triazine ring as electron accepting platform, and dipyridine amine as coordinating unit, formulated as $TTF_2$-tz-dpa (**1**) and TTF-tz-$dpa_2$ (**2**). The two ligands exhibit intramolecular charge transfer, evidenced experimentally and theoretically, from TTF toward the triazine unit. First metal coordination experiments afforded a neutral Zn(II) complex for **1**, while the ligand **2** provided a neutral dinuclear and a discrete tetracationic dimeric Zn(II) complexes, all of them thoroughly structurally analyzed. In the latter the occurrence of anion-$\pi$ supramolecular interactions has been evidenced, through the establishment of short Cl···triazine and perchlorate···triazine contacts. The electrochemical study of the ligands and the zinc neutral complexes suggests that these compounds are useful candidates for the preparation of radical cation salts. Although numerous TTF based ligands and complexes have been described to date,[22] those containing also a donor−acceptor system with tunable ICT, as the ligands **1** and **2**, are still rather rare.[39] Moreover, the presence of the electron poor triazine ring for the first time in the structure of TTF ligands makes possible the establishment of $\pi$-anion interactions in the solid state and their interplay with other supramolecular interactions, as well as their tuning with the TTF oxidation state. Having proven the coordination propensity of the new ligands, further studies will deal with the synthesis and properties of metal complexes containing either magnetic ions, to associate conductivity and magnetism in radical cation salts,[21] or with the switching of the photophysical properties of the ligands and complexes, since nitrogen rich aromatic compounds are often photoactive.

## EXPERIMENTAL SECTION

**General Procedures.** Elemental (C, H, and N) analyses were performed on a Thermo-Scientific Flash 2000 Organic Elemental Analyzer. NMR spectra were recorded on a Bruker Avance DRX 300 spectrometer operating at 300 MHz for $^1$H and 75 MHz for $^{13}$C. Chemical shifts are expressed in parts per million (ppm) downfield from external TMS, and the coupling constants are expressed in hertz (Hz). The following abbreviations are used: s, singlet; d, doublet. The IR spectra were recorded on ATR BRUKER VERTEX 70 spectrophotometer in the 4000−400 $cm^{-1}$ range. MALDI- TOF and ESI MS spectra were recorded on a Bruker Biflex-IIITM (equipped with a 337 nm N2 laser) and a Bruker Esquire 3000 plus apparatus, respectively. UV−vis spectra were recorded in solution using a Lambda 19 PERKIN ELMER Spectrometer. Unless mentioned otherwise, all the chemicals were purchased from commercial sources and were used as received. The perchlorate salts were manipulated with great care, and only small amounts were used. The precursors $Cl_2$-tz-dpa (2,4-dichloro[6-(dipyridin-2-ylamino)]-1,3,5-triazine) and Cl-tz-$dpa_2$ (2-chloro-[4,6-(dipyridin-2-ylamino)]-1,3,5-triazine)) were prepared as described elsewhere.[2a]

**Syntheses. (2,4-Bis-tetrathiafulvalene[6-(dipyridin-2′-ylamino)]-1,3,5-triazine) $TTF_2$-tz-dpa (1).** To a mixture of $Cl_2$-tz-dpa (0.127 g, 0.4 mmol) and TTF-$SnMe_3$ (0.323 g, 0.88 mmol) in dry toluene (20 mL), a catalytic amount of $Pd(PPh_3)_4$ (0.152 g, 0.132 mmol) was added. The resulting mixture was refluxed under argon overnight. The solvent was removed under reduced pressure, and the residue was purified by column chromatography (dichloromethane/hexane = 2:1) to afford 0.191 g of **1** as a dark mauve solid. Yield: 73%. $\lambda_{max}(CH_3CN)$/nm 299 ($\varepsilon$/$dm^3$ $mol^{-1}$ $cm^{-1}$ 11110), 316 sh, 504 (1010). $^1$H NMR ($CD_2Cl_2$, 25 °C): $\delta$ = 8.48 (ddd, $^3J$ = 4.9, $^4J$ = 1.9, $^5J$ = 0.7, 2H, py-H), 7.92 (ddd, $^3J$ = 8.2, $^4J$ = 1.9, 2H, py-H), 7.67 (dd, $^3J$ = 8.2, $^4J$ = 0.8, 2H, py-H), 7.65 (s, 2H, CH═C−C═N), 7.31 (ddd, $^3J$ = 4.9, $^4J$ = 2.4, $^5J$ = 0.9, 2H, py-H), 6.43 (d, $^3J$ = 6.5, 2H, CH═CH), 6.40 (d, $^3J$ = 6.5, 2H, CH═CH). $^{13}$C NMR ($CD_2Cl_2$, 25 °C): $\delta$ = 164.7, 154.4, 154.3, 153.6, 148.6, 137.8, 135.4, 129.9, 125.0, 122.8, 121.9, 119.3, 118.9, 112.8, 108.5. Selected IR bands ($cm^{-1}$): 1587, 1568, 1500, 1451, 1424, 1364, 1295, 874, 840, 797, 777, 730, 639. MALDI-TOF MS calcd: $m/z$ = 653.9, found: $m/z$ 653.4. Anal. Calcd. for $C_{25}H_{14}N_6S_8$: C, 45.85; H, 2.15; N, 12.83. Found C, 45.80; H, 2.27; N, 12.15.

**(2-Tetrathiafulvalene[4,6-bis-(dipyridin-2′-ylamino)]-1,3,5-triazine) TTF-tz-$dpa_2$ (2).** Cl-tz-$dpa_2$ (0.272 g, 0.6 mmol), TTF-$SnMe_3$ (0.242 g, 0.66 mmol) and $Pd(PPh_3)_4$ (0.114 g, 0.1 mmol) in toluene (30 mL) were refluxed overnight under argon. The solvent was removed under reduced pressure and the residue was purified by column chromatography (dichloromethane/hexane =4:1) to afford 0.302 g of **2**, a dark mauve solid. Yield: 81%. $\lambda_{max}(CH_3CN)$/nm 286 ($\varepsilon$/$dm^3$ $mol^{-1}$ $cm^{-1}$ 45400), 317 sh, 473 (3050). $^1$H NMR ([$D_6$]DMSO, 25 °C): $\delta$ = 8.29 (ddd, $^3J$ = 4.8, $^4J$ = 1.9, $^5J$ = 0.8, 4H, py-H), 7.83 (ddd, $^3J$ = 8.2, $^4J$ = 1.9, 4H, py-H), 7.57 (dd, $^3J$ = 8.12, $^4J$ = 0.8, 4H, py-H), 7.45 (s, 1H, CH═C−C═N), 7.21 (ddd, $^3J$ = 4.9, $^4J$ = 2.4, $^5J$ = 1.0, 4H, py-H), 6.73 (d, $^3J$ = 6.4, 1H, CH═CH), 6.71 (d, $^3J$ = 6.4 Hz, 1H, CH═CH). $^{13}$C NMR ([$D_6$]DMSO): $\delta$ = 165.4, 164.9, 154.8, 148.5, 137.3, 136.1, 133.5, 132.0, 132.0, 128.6, 128.5,


dx.doi.org/10.1021/ic301117h | Inorg. Chem. 2012, 51, 8545−8556

**Table 7. Crystal Data and Structure Refinement for 1 and 3−5**

| compound | 1 | 3 | 4 | 5 |
|---|---|---|---|---|
| empirical formula | $C_{25}H_{14}N_6S_8$ | $C_{25}H_{14}Cl_2N_6S_8Zn$ | $C_{29}H_{19}Cl_4N_9OS_4Zn_2$ | $C_{58}H_{38}Cl_4N_{18}O_{24}S_8Zn_2$ |
| fw | 654.90 | 791.17 | 910.31 | 1900.08 |
| $T$ (K) | 293(2) | 293(2) | 293(2) | 293(2) |
| wavelength (Å) | 0.71073 | 0.71073 | 0.71073 | 0.71073 |
| cryst syst | monoclinic | triclinic | triclinic | monoclinic |
| space group | $P2_1/a$ | $P\bar{1}$ | $P\bar{1}$ | $P2_1/n$ |
| $a$ (Å) | 8.7110(10) | 8.9316(6) | 11.4652(15) | 11.349(4) |
| $b$ (Å) | 29.080(5) | 13.2988(12) | 13.1499(19) | 16.1960(16) |
| $c$ (Å) | 10.925(2) | 13.6163(11) | 13.3930(16) | 21.525(4) |
| $\alpha$ (deg) | 90 | 83.468(6) | 66.093(9) | 90 |
| $\beta$ (deg) | 96.941(11) | 82.751(6) | 81.184(10) | 91.132(18) |
| $\gamma$ (deg) | 90 | 85.655(7) | 76.518(10) | 90 |
| $V$ (Å$^3$) | 2747.2(8) | 1590.9(2) | 1791.2(4) | 3955.9(14) |
| $Z$ | 4 | 2 | 2 | 2 |
| $D_c$ (g cm$^{-3}$) | 1.583 | 1.652 | 1.688 | 1.595 |
| abs coeff (mm$^{-1}$) | 0.680 | 1.494 | 1.911 | 1.037 |
| $F$(000) | 1336 | 796 | 912 | 1920 |
| cryst size (mm$^3$) | 0.5 × 0.1 × 0.1 | 0.5 × 0.2 × 0.1 | 0.3 × 0.2 × 0.2 | 0.2 × 0.1 × 0.08 |
| $\theta$ range for data collection (deg) | 3.37−27.51 | 3.09−27.49 | 2.56−27.49 | 2.40−27.4 |
| reflns collected | 6217 | 7280 | 7744 | 8808 |
| indep reflns | 3084 | 4611 | 5070 | 4815 |
| completeness (%) | 98.4 | 99.0 | 99.0 | 97.9 |
| refinement method | full-matrix least-squares on $F^2$ | full-matrix least-squares on $F^2$ | full-matrix least-squares on $F^2$ | full-matrix least-squares on $F^2$ |
| data/restraints/param | 6217/0/352 | 7280/0/514 | 7744/0/442 | 8808/0/514 |
| GOF on $F^2$ | 1.039 | 1.035 | 1.04 | 1.033 |
| final $R$ indices [$I > 2\sigma(I)$] | R1 = 0.0676 | R1 = 0.0501 | R1 = 0.0544 | R1 = 0.0677 |
| | wR2 = 0.0858 | wR2 = 0.1083 | wR2 = 0.1299 | wR2 = 0.1680 |
| $R$ indices (all data) | R1 = 0.1087 | R1 = 0.0995 | R1 = 0.0954 | R1 = 0.1380 |
| | wR2 = 0.1656 | wR2 = 0.1285 | wR2 = 0.1565 | wR2 = 0.2258 |
| largest diff. peak and hole (e Å$^{-3}$) | 0.350 and −0.369 | 0.545 and −0.382 | 0.903 and −1.076 | 0.72 and −0.544 |

128.2, 122.7, 121.3, 119.3, 119.0, 112.2, 108.9. Selected IR bands (cm$^{-1}$): 1587, 1523, 1459, 1429, 1366, 1295, 1252, 1189, 1149, 1118, 1049, 995, 840, 775, 743, 720, 693, 665, 649. MALDI-TOF MS calcd: $m/z$ = 621.06, found: $m/z$ 622.5. Anal. Calcd. for $C_{29}H_{19}N_9S_4$: C, 56.02; H, 3.08; N, 20.27. Found C, 57.00; H, 3.29; N, 19.91.

**Complex 3.** In a test tube, a solution of **1** (13 mg, 0.02 mmol) in $CH_2Cl_2$ (2 mL) was mixed with a solution of $ZnCl_2$ (2.7 mg, 0.02 mmol) in $CH_3CN$ (1 mL) and ultrasonicated for 2 min. On top of the resulting solution a layer of 1:1 diethylether: hexane mixture was added, which led to the formation of single crystals of **3** after 4 days. Yield: 12 mg (76%). $^1$H NMR ([D$_6$]DMSO, 25 °C): $\delta$ = 8.38 (ddd, $^3J$ = 4.9, $^4J$ = 1.9, $^5J$ = 0.8, 2H, py-H), 7.92 (ddd, $^3J$ = 8.2, $^4J$ = 1.9, 2H, py-H), 7.89 (s, 2H, CH═C−C═N), 7.68 (dd, $^3J$ = 8.1, $^4J$ = 0.9, 2H, py-H), 7.32 (ddd, $^3J$ = 6.3, $^4J$ = 2.4, $^5J$ = 1.0, 2H, py-H), 6.76 (d, $^3J$ = 6.4 Hz, 2H, CH═CH), 6.73 (d, $^3J$ = 6.43 Hz, 2H, CH═CH). Selected IR bands (cm$^{-1}$): 1605, 1504, 1470, 1433, 1367, 1299, 1252, 1194, 1152, 1049, 1027, 843, 790, 778, 727, 674, 647. ESI-MS: $m/z$ (M-2Cl: 717, M-Cl: 752) Anal. Calcd. for $C_{25}H_{14}Cl_2N_6S_8Zn$: C, 37.95; H, 1.78; N, 10.62. Found C, 37.71; H, 2.03; N, 10.14.

**Complex 4.** In a test tube, a solution of **2** (12.42 mg, 0.02 mmol) in $CH_2Cl_2$ (2 mL) was mixed with a solution of $ZnCl_2$ (5.44 mg, 0.04 mmol) in $CH_3CN$ (1 mL) and ultrasonicated for 2 min. On top of the resulting solution a layer of 1:1 v/v diethylether:hexane mixture was added, which led to the formation of single crystals of **4** after 5 days. Yield: 14.6 mg (80%). $^1$H NMR ([D$_6$]DMSO, 25 °C): $\delta$ = 8.29 (ddd, $^3J$ = 4.9 Hz, $^4J$ = 1.9, $^5J$ = 0.8, 4H, py-H), 7.82 (ddd, $^3J$ = 8.2, $^4J$ = 1.9, 4H, py-H), 7.56 (d, $^3J$ = 8.1, $^4J$ = 0.9, 4H, py-H),7.45 (s, 1H, CH═C−C═N), 7.21 (ddd, $^3J$ = 7.4, $^4J$ = 2.4, $^5J$ = 1.0, 4H, py-H), 6.73 (d, $^3J$ = 6.4, 1H, CH═CH), 6.70 (d, $^3J$ = 6.4, 1H, CH═CH). Selected IR bands (cm$^{-1}$): 3071, 1605, 1534, 1465, 1376, 1301, 1251, 1155, 1052, 1028, 841, 771, 757, 660. ESI-MS: $m/z$ (M-2Cl: 383). Anal. Calcd. for $C_{29}H_{21}Cl_4N_9OS_4Zn_2$: C, 38.17; H, 2.32; N, 13.82. Found C, 39.44; H, 2.43; N, 13.71.

**Complex 5.** In a test tube, a solution of **2** (12.42 mg, 0.02 mmol) in $CH_2Cl_2$ (2 mL) was mixed with a solution of $Zn(ClO_4)_2{\cdot}6H_2O$ (7.44 mg, 0.02 mmol) in $CH_3CN$ (1 mL) and ultrasonicated for 2 min. Single crystals of **5** were grown by liquid−liquid slow diffusion of the resulting solution into a layer of diethylether. Yield: 15 mg (81%). $^1$H NMR ([D$_6$]DMSO, 25 °C): $\delta$ = 8.31 (ddd, $^3J$ = 4.8, $^4J$ = 1.9, $^5J$ = 0.7, 4H, py-H), 7.85 (ddd, $^3J$ = 7.4, $^4J$ = 1.9, 4H, py-H), 7.59 (d, $^3J$ = 8.2, 4H, py-H), 7.47 (s, 1H, CH═C−C═N), 7.23 (ddd, $^3J$ = 7.3, $^4J$ = 2.4, $^5J$ = 0.9, 4H, py-H), 6.74 (d, $^3J$ = 6.4, 1H, CH═CH), 6.72 (d, $^3J$ = 6.4, 1H, CH═CH). Selected IR bands (cm$^{-1}$): 3510, 1606, 1531, 1469, 1371, 1299, 1252, 1194, 1152, 1049, 1027, 843, 790, 778, 727, 674, 647. ESI-MS: $m/z$ (M-4H$_2$O-ClO$_4$: 1673), $m/z$ (M-4H$_2$O-2ClO$_4$: 784). Anal. Calcd. for $C_{58}H_{54}Cl_4N_{18}O_{24}S_8Zn_2$: C, 36.35; H, 2.84; N, 13.16. Found C, 35.84; H, 2.52; N, 13.13.

**X-ray Structure Determinations.** Details about data collection and solution refinement are given in Table 7. Experimental X-ray diffraction data on single crystals were collected at room temperature using a Bruker Nonius Kappa CCD diffractometer operating with a Mo−K$\alpha$ ($\lambda$ = 0.71073 Å) X-ray tube with a graphite monochromator. The structures were solved (SHELXS-97) by direct methods and refined (SHELXL-97) by full-matrix least-squares procedures on $F^2$.[40] All non-H atoms of the donor molecules were refined anisotropically, and hydrogen atoms were introduced at calculated positions (riding model), included in structure factor calculations but not refined. Crystallographic data for the structures have been deposited in the Cambridge Crystallographic Data Centre, deposition numbers CCDC 882259 (**1**), CCDC 882260 (**3**), CCDC 882261 (**4**), and CCDC 882262 (**5**).

**Electrochemical studies.** Cyclic voltammetry measurements were performed in a three-electrode cell equipped with a platinum


dx.doi.org/10.1021/ic301117h | Inorg. Chem. 2012, 51, 8545−8556

millielectrode, a platinum wire counter-electrode, and a silver wire used as quasi-reference electrode. The electrochemical experiments were carried out under dry and oxygen-free atmosphere ($H_2O$ < 1 ppm, $O_2$ < 1 ppm) DCM/ACN 50/50 (ca. 0.5 mM) with $Bu_4NPF_6$ (TBAP) (0.1 M) as supporting electrolyte. The voltammograms were recorded on an EGG PAR 273A potentiostat with positive feedback compensation. On the basis of repeated measurements, absolute errors on potentials were estimated around ±5 mV.

**Theoretical Calculations.** Optimized geometries, starting from the X-ray data, have been obtained with the Gaussian09 package[41] at the DFT level of theory. The PBE0 functional[42] has been used. Vibrational frequency calculations performed at the optimized structures at the same level of theory yielded only positive values. TD DFT calculations for the first 20 singlet excited states have been performed at the same level of theory at the equilibrium geometries.

## ■ ASSOCIATED CONTENT

### Supporting Information

X-ray analysis details, CV data, UV−vis spectra, and details of the theoretical calculations. This material is available free of charge via the Internet at http://pubs.acs.org.

## ■ AUTHOR INFORMATION


### Corresponding Author

*Fax: (+33)02 41 73 54 05. Phone: (+33)02 41 73 54 92. E-mail: abdelkrim.elghayoury@univ-angers.fr (A.E.-G.), narcis.avarvari@univ-angers.fr (N.A.).


### Notes

The authors declare no competing financial interest.

## ■ ACKNOWLEDGMENTS

Financial support from the CNRS, the University of Angers, the Region Pays de la Loire (grant for D.B.) and from the National Agency for Research (ANR, Project 09-BLAN-0045-01) is gratefully acknowledged. Flavia Pop is acknowledged for help with the synthesis of the ligands. Olivier Alévêque is acknowledged for help with CV measurements.

## ■ REFERENCES


(1) (a) Bartholomew, D. *1,3,5-Triazines, In Comprehensive heterocyclic Chemistry II*; Boulton, A. J., Ed.; Pergamon: Oxford, U.K., 1996; Vol. *6*. (b) Giacomelli, G.; Porcheddu, A.; Luca, L. D. *Curr. Org. Chem.* **2004**, *15*, 1497−1519.

(2) (a) de Hoog, P.; Gamez, P.; Driessen, W. L.; Reedijk, J. *Tetrahedron Lett.* **2002**, *43*, 6783−6786. (b) Steffensen, M. B.; Simanek, E. E. *Angew. Chem., Int. Ed.* **2004**, *43*, 5178−5180. (c) Wang, M.-X.; Yang, H.-B. *J. Am. Chem. Soc.* **2004**, *126*, 15412−15422.

(3) (a) Blotny, G. *Tetrahedron* **2006**, *62*, 9507−9522. (b) Kumar, A.; Menon, S. K. *Eur. J. Med. Chem.* **209**, *44*, 2178−2183.

(4) Fink, R.; Frenz, C.; Thelakkat, M.; Schmidt, H.-W. *Macromolecules* **1997**, *30*, 8177−8181.

(5) Wang, W.; Sun, H.; Kaifer, A. E. *Org. Lett.* **2007**, *9*, 2657−2660.

(6) Chérioux, F.; Maillotte, H.; Audeberta, P.; Zyss, J. *Chem. Commun.* **1999**, 2083−2084.

(7) Cui, Y.-Z.; Fang, Q.; Xue, G.; Xu, G.-B.; Yin, L.; Yu, W.-T. *Chem. Lett.* **2005**, *34*, 644−645.

(8) (a) Glaser, T.; Lügger, T.; Fröhlich, R. *Eur. J. Inorg. Chem.* **2004**, 394−400. (b) Selby, T. D.; Stickley, K. R.; Blackstock, S. C. *Org. Lett.* **2000**, *2*, 171−174.

(9) (a) Abrahams, B. F.; Batten, S. R.; Grannas, M. J.; Hamit, H.; Hoskins, B. F.; Robson, R. *Angew. Chem., Int. Ed.* **1999**, *38*, 1475−1477. (b) Biradha, K.; Fujita, M. *Angew. Chem., Int. Ed.* **2002**, *41*, 3392−3395. (c) Kumazawa, K.; Biradha, K.; Kusukawa, T.; Okano, T.; Fujita, M. *Angew. Chem., Int. Ed.* **2003**, *42*, 3909−3913. (d) Ohmori, O.; Kawano, M.; Fujita, M. *J. Am. Chem. Soc.* **2004**, *126*, 16292−16293. (e) Dinolfo, P. H.; Coropceanu, V.; Brédas, J.-L.; Hupp, J. T. *J. Am. Chem. Soc.* **2006**, *128*, 12592−12593. (f) Lear, B. J.; Kubiak, C. P. *Inorg. Chem.* **2006**, *45*, 7041−7043. (g) Ono, K.; Yoshizawa, M.; Kato, T.; Watanabe, K.; Fujita, M. *J. Am. Chem. Soc.* **2007**, *46*, 1803−1806. (h) Li, M.-X.; Miao, Z.-X.; Shao, M.; Liang, S.-W.; Zhu, S.-R. *Inorg. Chem.* **2008**, *47*, 4481−4489.

(10) (a) Gamez, P.; de Hoog, P.; Roubeau, O.; Lutz, M.; Driessen, W. L.; Spek, A. L.; Reedijk, J. *Chem. Commun.* **2002**, 1488−1489. (b) Demeshko, S.; Leibeling, G.; Dechert, S.; Meyer, F. *Dalton Trans.* **2004**, 3782−3787. (c) Demeshko, S.; Dechert, S.; Meyer, F. *J. Am. Chem. Soc.* **2004**, *126*, 4508−4509. (d) Quesada, M.; Monrabal, M.; Aromi, G.; de la Peña-O'Shea, V. A.; Gich, M.; Molins, E.; Roubeau, O.; Teat, S. J.; MacLean, E. J.; Gamez, P.; Reedijk, J. *J. Mater. Chem.* **2006**, *16*, 2669−2676. (e) Casellas, H.; Roubeau, O.; Teat, S. J.; Masciocchi, N.; Galli, S.; Sironi, A.; Gamez, P.; Reedijk, J. *Inorg. Chem.* **2007**, *46*, 4583−4591. (f) Barrios, L. A.; Aromi, G.; Frontera, A.; Quinonero, D.; Deya, P. M.; Gamez, P.; Roubeau, O.; Shotton, E. J.; Teat, S. J. *Inorg. Chem.* **2008**, *47*, 5873−5881. (g) Yuste, C.; Canadillas-Delgado, L.; Labrador, A.; Delgado, F. S.; Ruiz-Pérez, C.; Lloret, F.; Julve, M. *Inorg. Chem.* **2009**, *48*, 6630−6640. (h) Wong, E.; Li, J.; Seward, C.; Wang, S. *Dalton Trans.* **2009**, 1776−1785. (i) Singh, A. K.; Yadav, M.; Pandey, R.; Kumar, P.; Pandey, D. S. *J. Organomet. Chem.* **2010**, *695*, 1932−1939. (j) Hajra, T.; Bera, J. K.; Chandrasekhar, V. *Inorg. Chim. Acta* **2011**, *372*, 53−61.

(11) (a) Maheswari, P. U.; Modec, B.; Pevec, A.; Kozlevčar, B.; Massera, C.; Gamez, P.; Reedijk, J. *Inorg. Chem.* **2006**, *45*, 6637−6645. (b) Götzke, L.; Gloe, K.; Jolliffe, K. A.; Lindoy, L. F.; Heine, A.; Doert, T.; Jäger, A.; Gloe, K. *Polyhedron* **2011**, *30*, 708−714. (c) Maheswari, P. U.; van Albada, G. A.; Modec, B.; Kozlevčar, B.; Reedijk, J. *J. Mol. Struct.* **2012**, *1013*, 36−38.

(12) (a) Metcalfe, C.; Spey, S.; Adams, H.; Thomas, J. A. *J. Chem. Soc., Dalton Trans.* **2002**, 4732−4739. (b) Polson, M. I. J.; Medlycott, E. A.; Hanan, G. S.; Mikelsons, L.; Taylor, N. J.; Watanabe, M.; Tanaka, Y.; Loiseau, F.; Passalacqua, R.; Campagna, S. *Chem.—Eur. J.* **2004**, *10*, 3640−3648.

(13) (a) Lerner, E. I.; Lippard, S. J. *J. Am. Chem. Soc.* **1976**, *98*, 5397−5398. (b) Lerner, E. I.; Lippard, S. J. *Inorg. Chem.* **1977**, *16*, 1546−1551. (c) Garcia, A. M.; Bassani, D. M.; Lehn, J.-M.; Baum, G.; Fenske, D. *Chem.—Eur. J.* **1999**, *5*, 1234−1238. (d) de Castro Gomes, D. C.; Stumpf, H. O.; Lloret, F.; Julve, M.; González, V.; Adams, H.; Thomas, J. A. *Inorg. Chim. Acta* **2005**, *358*, 1113−1124.

(14) Yang, Q.-Y.; Zheng, S.-R.; Yang, R.; Pan, M.; Cao, R.; Su, C.-Y. *CrystEngComm* **2009**, *11*, 680−685.

(15) Behl, M.; Zentel, R. *Macromol. Chem. Phys.* **2004**, *205*, 1633−1643.

(16) (a) Sesto, R. E. D.; Botoshansky, M.; Kaftory, M.; Arifa, A. M.; Miller, J. S. *CrystEngComm* **2002**, *4*, 117−120. (b) Yoshizawa, M.; Kumazawa, K.; Fujita, M. *J. Am. Chem. Soc.* **2005**, *127*, 13456−43457. (c) Riobé, F.; Grosshans, P.; Sidorenkova, H.; Geoffroy, M.; Avarvari, N. *Chem.—Eur. J.* **2009**, *15*, 380−387.

(17) (a) Mascal, M.; Armstrong, A.; Bartberger, M. D. *J. Am. Chem. Soc.* **2002**, *124*, 6274−6276. (b) de Hoog, P.; Gamez, P.; Mutikainen, I.; Turpeinen, U.; Reedijk, J. *Angew. Chem., Int. Ed.* **2004**, *13*, 5815−5817.

(18) Garcia, A.; Insuasty, B.; Herranz, M.; Martinez-Alvarez, R.; Martin, N. *Org. Lett.* **2009**, *11*, 5398−5401.

(19) (a) Segura, J. L.; Martin, N. *Angew. Chem., Int. Ed.* **2001**, *40*, 1372−1409. (b) Canevet, D.; Salle, M.; Zhang, G. X.; Zhang, D. Q.; Zhu, D. B. *Chem. Commun.* **2009**, 2245−2269.

(20) (a) Williams, J. M.; Ferraro, J. R.; Thorn, R. J.; Carlson, K. D.; Geiser, U.; Wang, H. H.; Kini, A. M.; Whangbo, M.-H.; Hall, P., Eds; *Organic Superconductors*; Prentice Hall: Englewood Cliffs, NJ, 1992. (b) Bryce, M. R.; Murphy, L. C. *Nature* **1984**, *309*, 119−126.

(21) (a) Coronado, E.; Day, P. *Chem. Rev.* **2004**, *104*, 5419−5448. (b) Ouahab, L.; Enoki, T. *Eur. J. Inorg. Chem.* **2004**, 933−941. (c) Avarvari, N.; Wallis, J. D. *J. Mater. Chem.* **2009**, *19*, 4061−4076.

(22) (a) Lorcy, D.; Bellec, N.; Fourmigué, M.; Avarvari, N. *Coord. Chem. Rev.* **2009**, *253*, 1398−1438. (b) Shatruk, M.; Ray, L. *Dalton Trans.* **2010**, *39*, 11105−11121.

(23) (a) Avarvari, N.; Martin, D.; Fourmigué, M. *J. Organomet. Chem.* **2002**, *643/644*, 292−300. (b) Pellon, P.; Gachot, G.; Le Bris, J.; Marchin, S.; Carlier, R.; Lorcy, D. *Inorg. Chem.* **2003**, *42*, 2056−2060. (c) Avarvari, N.; Fourmigué, M. *Chem. Commun.* **2004**, 1300−1301. (d) Réthoré, C.; Fourmigué, M.; Avarvari, N. *Chem. Commun.* **2004**, 1384−1385. (e) Devic, T.; Batail, P.; Fourmigué, M.; Avarvari, N. *Inorg. Chem.* **2004**, *43*, 3136−3141. (f) Gouverd, C.; Biaso, F.; Cataldo, L.; Berclaz, T.; Geoffroy, M.; Levillain, E.; Avarvari, N.; Fourmigué, M.; Sauvage, F. X.; Wartelle, C. *Phys. Chem. Chem. Phys.* **2005**, *7*, 85−93. (g) Avarvari, N.; Fourmigué, M. *Chem. Commun.* **2004**, 2794−2795. (h) Fourmigué, M.; Uzelmeier, C. E.; Boubekeur, K.; Bartley, S. L.; Dunbar, K. R. *J. Organomet. Chem.* **1997**, *529*, 343−350. (i) Smucker, B. W.; Dunbar, K. R. *J. Chem. Soc., Dalton Trans.* **2000**, 1309−1315. (j) Avarvari, N.; Kiracki, K.; Llusar, R.; Polo, V.; Sorribes, I.; Vicent, C. *Inorg. Chem.* **2010**, *49*, 1894−1904.

(24) (a) Réthoré, C.; Fourmigué, M.; Avarvari, N. *Tetrahedron* **2005**, *61*, 10935−10942. (b) Madalan, A. M.; Réthoré, C.; Avarvari, N. *Inorg. Chim. Acta* **2007**, *360*, 233−240. (c) Riobé, F.; Avarvari, N. *Chem. Commun.* **2009**, 3753−3755. (d) Riobé, F.; Avarvari, N. *Coord. Chem. Rev.* **2010**, *254*, 1523−1533.

(25) Kobayashi, A.; Fujiwara, E.; Kobayashi, H. *Chem. Rev.* **2004**, *104*, 5243−5264.

(26) Massue, J.; Bellec, N.; Chopin, S.; Levillain, E.; Roisnel, T.; Clérac, R.; Lorcy, D. *Inorg. Chem.* **2005**, *44*, 8740−8748.

(27) (a) Setifi, F.; Ouahab, L.; Golhen, S.; Yoshida, Y.; Saito, G. *Inorg. Chem.* **2003**, *42*, 1791−1793. (b) Liu, S.-X.; Dolder, S.; Franz, P.; Neels, A.; Stoeckli-Evans, H.; Decurtins, S. *Inorg. Chem.* **2003**, *42*, 4801−4803. (c) Devic, T.; Avarvari, N.; Batail, P. *Chem.—Eur. J.* **2004**, *10*, 3697−3707. (d) Balandier, J.-Y.; Chas, M.; Goeb, S.; Dron, P. I.; Rondeau, D.; Belyasmine, A.; Gallego, N.; Sallé, M. *New. J. Chem.* **2011**, *35*, 165−168. (e) Gavrilenko, K. S.; Le Gal, Y.; Cador, O.; Golhen, S.; Ouahab, L. *Chem. Commun.* **2007**, 280−282. (f) Geng, Y.; Wang, X.-J.; Chen, B.; Xue, H.; Zhao, Y.-P.; Lee, S.; Tung, C.-H.; Wu, L.-Z. *Chem.—Eur. J.* **2009**, *15*, 5124−5129. (g) Kolotilov, S. V.; Cador, O.; Pointillart, F.; Golhen, S.; Le Gal, Y.; Gavrilenko, K. S.; Ouahab, L. *J. Mater. Chem.* **2010**, *20*, 9505−9514. (h) Liu, S.-X.; Ambrus, C.; Dolder, S.; Neels, A.; Decurtins, S. *Inorg. Chem.* **2006**, *45*, 9622−9624. (i) Devic, T.; Batail, P.; Avarvari, N. *Chem. Commun.* **2004**, 1538−1539.

(28) Devic, T.; Rondeau, D.; Sahin, Y.; Levillain, E.; Clérac, R.; Batail, P.; Avarvari, N. *Dalton Trans.* **2006**, 1331−1337.

(29) (a) Chahma, M.; Hassan, N.; Alberola, A.; Stoeckli-Evans, H.; Pilkington, M. *Inorg. Chem.* **2007**, *46*, 3807−3809. (b) Qin, J.; Qian, C.-X.; Zhou, N.; Zhu, R.-M.; Li, Y.-Z.; Zuo, J.-L.; You, X.-Z. *Eur. J. Inorg. Chem.* **2012**, 234−245. (c) Nita, G.; Branzea, D.; Pop, F.; El-Ghayoury, A.; Avarvari, N. *Crystals* **2012**, *2*, 338−348. (d) Wu, J.-C.; Liu, S.-X.; Keene, T. D.; Neels, A.; Mereacre, V.; Powell, A. K.; Decurtins, S. *Inorg. Chem.* **2008**, *47*, 3452−3459.

(30) Aakeröy, C. B.; Champness, N. R.; Janiak, C. *CrystEngComm* **2010**, *12*, 22−43.

(31) Pang, J.; Marcotte, E. J.-P.; Seward, C.; Brown, R. S.; Wang, S. *Angew. Chem., Int. Ed.* **2001**, *40*, 4042−4045.

(32) Novaković, S. B.; Fraisse, B.; Bogdanović, G. A.; Spasojević- de Biré, A. *Cryst. Growth Des.* **2007**, *7*, 191−195.

(33) Janiak, C. *J. Chem. Soc., Dalton Trans.* **2000**, 3885−3896.

(34) (a) Habib, H. A.; Hoffmann, A.; Höppe, H. A.; Steinfeld, G.; Janiak, C. *Inorg. Chem.* **2009**, *48*, 2166−2180. (b) Wisser, B.; Janiak, C. *Z. Anorg. Allg. Chem.* **2007**, *633*, 1796−1800.

(35) Addison, A. W.; Rao, T. N.; Reedijk, J.; van Rijn, J.; Verschoor, G. C. *J. Chem. Soc., Dalton Trans.* **1984**, 1349−1356.

(36) (a) Hunter, C. A.; Sanders, J. K. M. *J. Am. Chem. Soc.* **1990**, *112*, 5525−5534. (b) Mooibroek, T. J.; Black, C. A.; Gamez, P.; Reedijk, J. *Cryst. Growth Des.* **2008**, *8*, 1082−1093. (c) Hay, B. P.; Bryantsev, V. S. *Chem. Commun.* **2008**, 2417−2428. (d) Gural'skiy, I. A.; Escudero, D.; Frontera, A.; Solntsev, P. V.; Rusanov, E. B.; Chernega, A. N.; Krautscheid, H.; Domasevitch, K. V. *Dalton Trans* **2009**, 2856−2864. (e) Berryman, O. B.; Johnson, D. W. *Chem. Commun.* **2009**, 3143−3153.

(37) Neville, S. M.; Leita, B. A.; Offermann, D. A.; Duriska, M. B.; Moubaraki, B.; Chapman, K. W.; Halder, G. J.; Murray, K. S. *Eur. J. Inorg. Chem.* **2007**, 1073−1085.

(38) Pang, J.; Tao, Y.; Freiberg, S.; Yang, X.-P.; D'Iorio, M.; Wang, S. *J. Mater. Chem.* **2002**, *12*, 206−212.

(39) (a) Dupont, N.; Ran, Y.-F.; Jia, H.-P.; Grilj, J.; Ding, J.; Liu, S.-X.; Decurtins, S.; Hauser, A. *Inorg. Chem.* **2011**, *50*, 3295−3303. (b) Ran, Y.-F.; Liu, S.-X.; Sereda, O.; Neels, A.; Decurtins, S. *Dalton Trans.* **2011**, *40*, 8193−8198.

(40) Sheldrick, G. M. *SHELXS-97, SHELXL-97, Programs for the Refinement of Crystal Structures*; University of Göttingen: Göttingen, Germany, 1996.

(41) Frisch, M. J.; Trucks, G. W.; Schlegel, H. B.; Scuseria, G. E.; Robb, M. A.; Cheeseman, J. R.; Scalmani, G.; Barone, V.; Mennucci, B.; Petersson, G. A.; Nakatsuji, H.; Caricato, M.; Li, X.; Hratchian, H. P.; Izmaylov, A. F.; Bloino, J.; Zheng, G.; Sonnenberg, J. L.; Hada, M.; Ehara, M.; Toyota, K.; Fukuda, R.; Hasegawa, J.; Ishida, M.; Nakajima, T.; Honda, Y.; Kitao, O.; Nakai, H.; Vreven, T.; Montgomery, J. A., Jr.; Peralta, J. E.; Ogliaro, F.; Bearpark, M.; Heyd, J. J.; Brothers, E.; Kudin, K. N.; Staroverov, V. N.; Kobayashi, R.; Normand, J.; Raghavachari, K.; Rendell, A.; Burant, J. C.; Iyengar, S. S.; Tomasi, J.; Cossi, M.; Rega, N.; Millam, J. M.; Klene, M.; Knox, J. E.; Cross, J. B.; Bakken, V.; Adamo, C.; Jaramillo, J.; Gomperts, R.; Stratmann, R. E.; Yazyev, O.; Austin, A. J.; Cammi, R.; Pomelli, C.; Ochterski, J. W.; Martin, R. L.; Morokuma, K.; Zakrzewski, V. G.; Voth, G. A.; Salvador, P.; Dannenberg, J. J.; Dapprich, S.; Daniels, A. D.; Farkas, Ö.; Foresman, J. B.; Ortiz, J. V.; Cioslowski, J.; Fox, D. J. *Gaussian 09*, Revision A.2; Gaussian, Inc.: Wallingford, CT, 2009.

(42) Adamo, C.; Barone, V. *J. Chem. Phys.* **1999**, *110*, 6158−6169.